Science Advances
AAAS

advances.sciencemag.org/cgi/content/full/5/4/eaav7959/DC1

Supplementary Materials for

Ultra-multiplexed analysis of single-cell dynamics reveals logic rules in differentiation

Ce Zhang, Hsiung-Lin Tu, Gengjie Jia, Tanzila Mukhtar, Verdon Taylor, Andrey Rzhetsky, Savaş Tay*

*Corresponding author. Email: tays@uchicago.edu

Published 3 April 2019, *Sci. Adv.* **5**, eaav7959 (2019)
DOI: 10.1126/sciadv.aav7959

The PDF file includes:

Other Supplementary Material for this manuscript includes the following:

(available at advances.sciencemag.org/cgi/content/full/5/4/eaav7959/DC1)

Table S1 (Microsoft Excel format). Microenvironment exposed to six single ligands and combinatorial and sequential ligand inputs (note: the order of the ligands in the table represents the order of ligands introduced into the microenvironments on daily bases).
Table S2 (Microsoft Excel format). Statistical analysis results associated with sequential and combinatorial inputs of six ligands based on cell count measurements and *Hes5* and *Dcx* expression level.
Movie S1 (.mov format). COMSOL simulation and time-lapse video of fluid exchange in a unit chamber on the chip.
Movie S2 (.avi format). Redistribution of GFP after medium exchange and all valves are closed.
Movie S3 (.mov format). Retrieval of adherent cells (3T3, left) and suspension-cultured cells (Jurkat, right) from the chip.
Movie S4 (.avi format). Stimulation of 3T3 cells by sinusoidal TNF-α inputs.
Movie S5 (.mov format). Cell tracking videos of NSC spheres (top) and monolayer (bottom).

Supplementary Information

Section S1. Temporal and spatial concentration distribution within the cell culture chambers

In this section, we describe the temporal and spatial concentration variations inside culture chambers, especially during ligand loading. Simulations in Fig. 1C shows that the concentration variations in the culture chambers are negligible during feeding/stimulation mode, and the steady-state concentration at the bottom of the culture chamber is stable and homogenous in both space and time (Fig. 1C and fig. S1, video S1 and S2). Diffusion is very efficient at the scale of our culture chambers (~100 μm), in which a steady state can be reached within few minutes. As such, delivery of nutrients and ligands is much faster compared to signaling events relevant to neural stem cell (NSC) differentiation, which typically take days.

The spatial and temporal concentration profiles are now characterized at various points within the chamber using the green fluorescent protein (GFP) as tracer (fig. S1). Notably, cells are cultured at bottom left corner of the culture well (Point 3), and the buffer layer (Point 1) is only used to load culture media. Point 2 is right above the cells. When a new signaling ligand is loaded into the chamber via point 1; the valves are closed, and then the ligand is transported to point 2 and then point 3 via diffusion. During our feeding/stimulation cycle, the concentration at point 2 (above cultured cells) is nearly unchanged during medium exchange with 1 mm/sec input flow rate, which is the value typically used in our experiments. This experimental result agrees well with our original

numerical simulation results (Fig. 1C, video S1 and S2). When all the valves are closed (i.e. medium exchange completed), signaling molecules and chemical stimuli diffuse to the bottom of culture chamber (Point 1) until an equilibrium is reached after 10 min (fig. S1D and S1E). Note that this timescale is much faster than the NSC processes we investigated here, which typically take one-to-few days to show sufficient changes in *Hes5* expression or cell proliferation. We therefore confirm that the temporal variations of signaling molecules are negligible within our culture chambers for the study of neural stem cells (NSCs) and other systems with similar time scales. Furthermore, the spatial distribution of molecules is homogenous after the steady state has been reached, i.e. there are no spatial gradients in the culture chambers (fig. S1D).

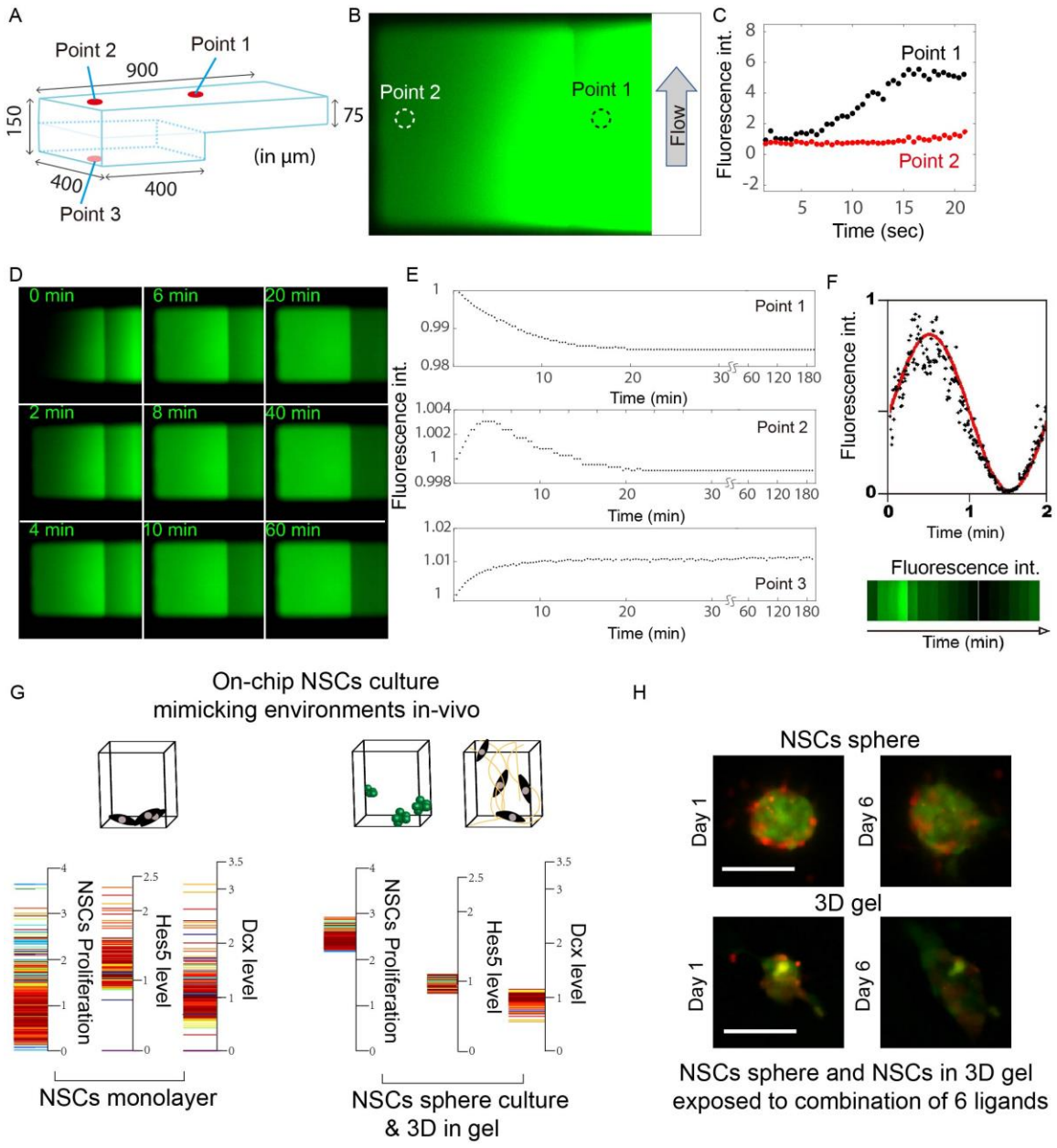

Fig. S1. Experimental characterization of concentration variations during medium exchange. (A) Temporal variation of Green Fluorescent Protein (GFP, PRO-687, ProSpec) fluorescence intensity are monitored at 3 positions in the chamber: Point 1 at the buffering layer, Point 2 at the top of the culture layer and Point 3 at the bottom of the culture chamber. (B) Fluorescent image of culture chamber at 100 seconds after the beginning of medium exchange. The input flow rate is 1 mm/sec with arrow indicating flow direction. (C) Temporal fluorescence intensity profiles at position 1 and 2 (indicated in Fig. B) demonstrate that GFP concentration is stable during medium exchange, suggesting no direct flow and the delivery of fluorescent molecules from Point 1 to Point 2 is accomplished through diffusion. (D) Snapshots of culture chamber at different time points after all valves are closed. Concentration of fluorescent molecules is high close to

inlet, and gradually diffuse to culture compartment after 6 min. Near-equilibrium is reached after approximately 7 min, and the spatial distribution of molecules becomes homogenous across the culture chamber. (E) After ~15 min, the concentrations are completely stabilized at all 3 points. (F) Sinusoidal wave generation shows that previous ligands can be completely removed within 1 minute from the culture chambers. A sinusoidal wave is generated by real-time mixing of GFP-fluorescence solution and DI water. In the upper panel, the fluorescence intensity in the cell culture chamber is plotted against time. In the lower panel, montage of snapshot images of the culture chamber during real-time medium exchange is shown. The media has been completely cleared from the culture chamber within 1 minute. (G) Signal induced variations in NSC cell count, *Hes5*-GFP and *Dcx*-RFP expression are plotted as bars indicating their intensities and values relative to the control experiments after 6 days of stimulation. The outcome of 2,400 experiments shows NSC cell counts, *Hes5* and *Dcx* level after 6 days of culture. NSC monolayer cell shows greater variation in all 3 categories as compared to neurospheres and 3D culture. (H) Fluorescence images of neurospheres and aggregates in 3D hydrogel after 6 days of stimulation with combination of all 6 ligands, *Jagged*, *DLL*, *EGF*, PACAP, *CXCL*, *PDGF*.

In order to diminish shear and to maintain a stable culture environment during medium exchange, we designed our chip so that fluid can be directed through a buffering layer and not directly over cells (Fig. 1C). Therefore, there is a quiescent zone at the bottom of the well, and residues can indeed remain if the chamber is not sufficiently flushed during media exchange cycles. We note that each condition in our culture wells are maintained by repeatedly refilling the chamber with fresh media and stimulation ligands every 5 min to 1 hour. Based on numerical simulation, each flushing cycle removes 80% of the original solution when 1mm/sec input flow rate is used (Fig. 1C). Each chamber is flushed for at least 20 times during one day of culture. As a result, the concentration of any previously used molecules goes down to 0.8% of the initial concentration after 3 cycles and ultimately to ~10^{-10} times after 20 cycles.

To further investigate this point, we generated a sinusoidal wave signal in the culture chamber to simulate cyclical media exchange (fig. S1F). The cell culture chamber is programed to be filled with different concentrations and mixtures of green fluorescent protein (GFP) and DI water. The chamber is then imaged continuously, and average GFP intensity is recorded. This experiment shows the residuals can be efficiently removed and there are no residuals from previous treatment in the culture chambers: The fluorescence intensity goes down to undetectable levels at the valley of the sine wave, showing that residue medium can be completely cleared within 1 minute (fig. S1F).

Section S2. Single 3T3 fibroblast cell culture and stimulation on chip

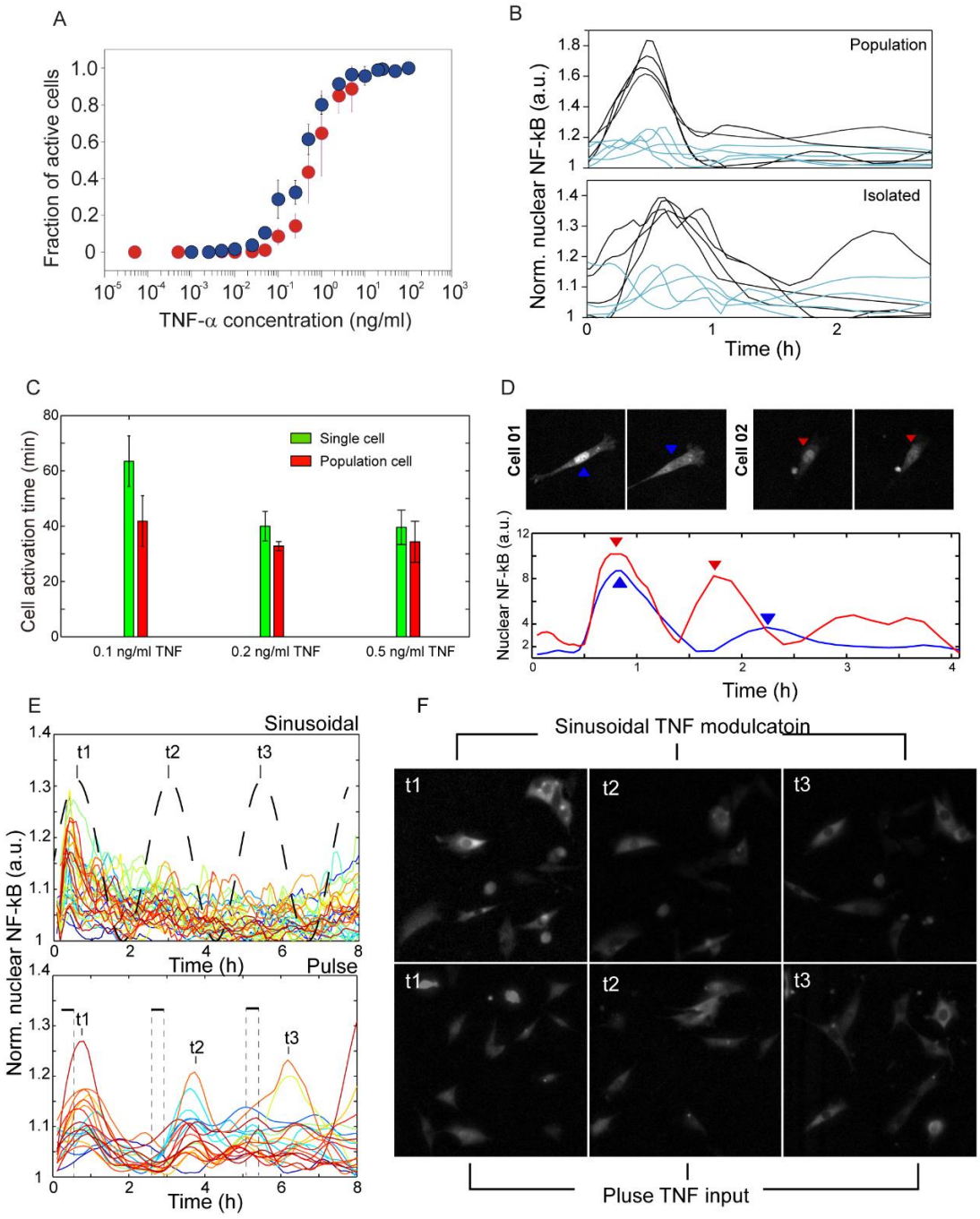

Fig. S2. Assessment of the microfluidic system for dynamical cell culture and NF-κB signaling. (A) Fraction of activated 3T3 cell at various TNF-alpha concentrations. Dilutions of TNF-alpha are performed through pipetting (blue circles), and on-chip

dilution using peristaltic pumps (red circles). (B) Single-cell NF-κB nuclear localization traces for active and non-activated cells. The blue traces show non-activated cells while the black curves show the activated cells. (C) Activation time of population and isolated single 3T3 cells at 0.1, 0.2 and 0.5 ng/ml TNF concentration respectively. (D) Fluorescence images and NF-κB nuclear localization traces of isolated single 3T3 cells showing oscillation following the first stimulation at 0.2 ng/ml TNF concentration. (E) Single-cell NF-κB nuclear localization traces for 3T3 cells in micro-environments with sinusoidal and pulsed TNF modulation. The maximum TNF concentration is 5 ng/ml in both cases. The sinusoidal signal is created by modulating the real-time TNF concentration through on-chip mixing, while the digital TNF pulses are provided by replacing each culture chamber with flash culture medium following 15-min TNF pulses. (F) Real-time fluorescent images of 3T3 cells during sinusoidal and pulse TNF stimulation.

Section S3. Culture and stimulation of human and mouse HSCs on chip

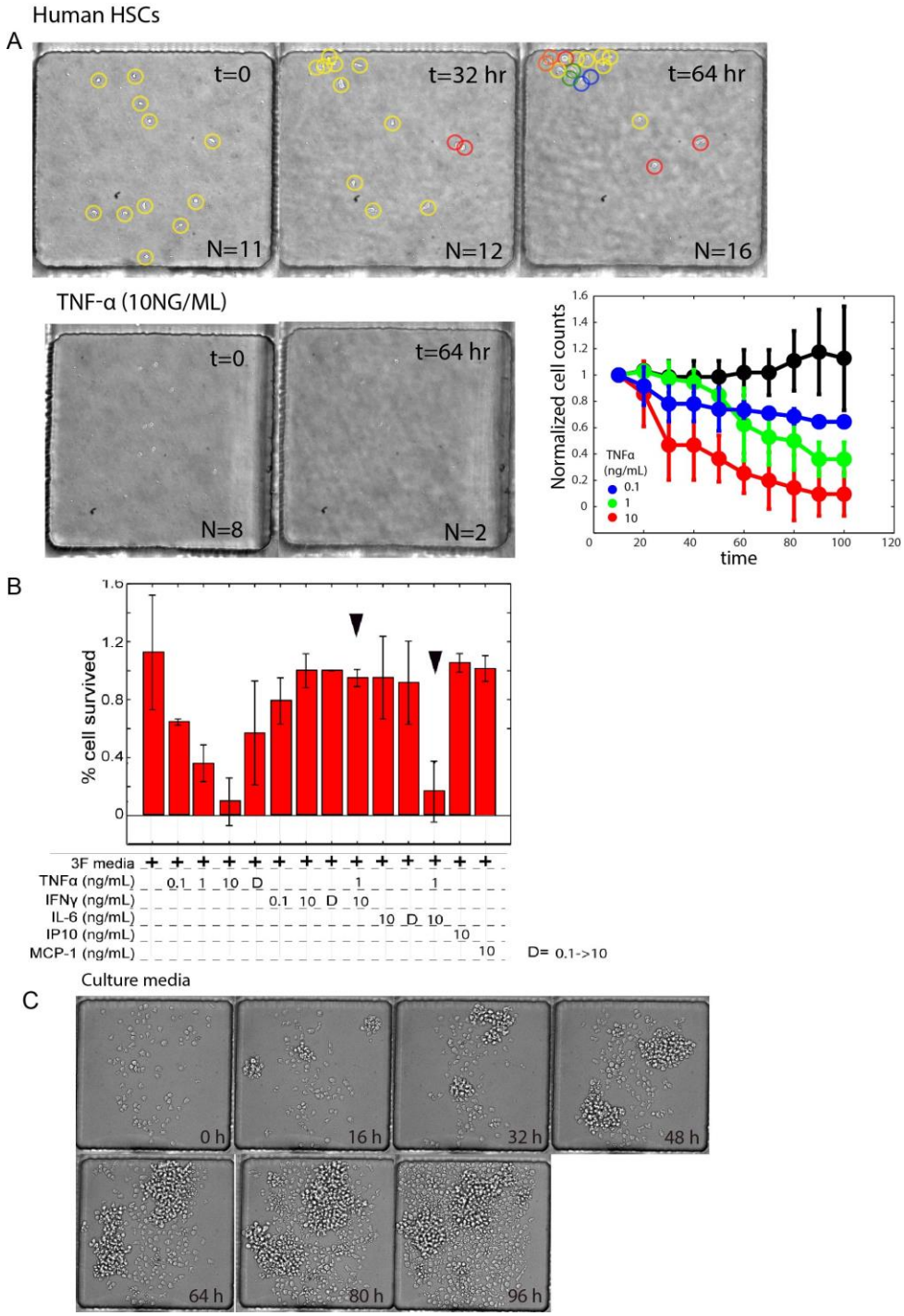

Fig. S3. **Culture and stimulation of human HSCs on chip.** (A) Long-term culture and TNF stimulation of human HSCs. Cells were cultured on the microfluidic device in the absence of TNF (control; top) and with 10 ng/ml TNF (bottom), for up to 5 days. Bottom

right panel shows relative cell numbers upon stimulation with TNF (black dot represents control experiment without TNF stimulation). N indicates cell numbers per chamber. (B) Long-term culture and TNF stimulation of human hematopoietic stem cells (HSCs). Cells were cultured on the microfluidic device in the absence (control) and presence of TNF for up to 5 days. The panel shows effect of TNF in the presence of other participating cytokines (IFNγ, IL-6, IP10 and MCP-1). TNF induces dosage-dependent death of human HSCs, and IFNγ neutralize TNF induced cell death. D represents dynamic cytokine inputs, daily variation between 0.1 and 10 ng/ml. (C) Culture of Jurkat cells in suspension mode for 4 days.

Section S4. Culture and stimulation of NSC spheres on chip

The cells located deep inside the neurospheres may not have access to the same conditions/growth factors as the cells outside due to limited transport of media and signaling molecules. These transport limitations can create dose effects for cells at different locations within the neurosphere. For example, in the application note of CellASIC ONix live cell analysis platform from Millipore, it is demonstrated that molecules like Sox2 and nestin antibodies cannot fully diffuse into the NSCs spheres, and stain only cells at the outer layer (https://www.sigmaaldrich.com/technical-documents/articles/biology/cellasic-onix-live-cell-analysis-platform-for-neural-stem-cell-microenvironment-control.html). Similarly, in our system we observe that mature, larger neurospheres are overall more resistant to stimulation with signaling molecules, suggesting limited transport when compared to smaller neurospheres (fig. S4A to S4E). Such limited transport is a common property of many 3D culture modalities such as cell aggregates and organoids. Nevertheless, 3D cell culture continues to attract significant attention due to its promise in mimicking tissue-like organization.

In detail, we observed that *Dcx*-high and *Hes5*-high cells self-organize into layered structures during neurosphere formation (fig. S4A to S4C). *Dcx*-high cells tend to stay at the periphery of the neurosphere. GFP-high cells form a densely packed inner-sphere. As a result, the *Dcx*-high cells are rapidly exposed to the stimuli, and *Hes5*-high ones at the core take longer time to respond to the ligands due to transport effects. This finding is also supported by the size dependence of neurospheres response to combinatorial stimulation with all 6 ligands. When the initial sphere size is small, *Hes5* positive NSCs

tend to die and overall *Hes5* level decreases in the neurosphere, which is consistent with the response of NSCs in monolayer culture (Fig. 2E and fig. S4D). But, when sphere size is large enough, neurospheres continue to grow and *Hes5* level remains high, similar to control experiments (Fig. 2). This shows that when neurosphere size is large, the cells at the core are better protected from environmental stimuli, and thus less responsive to dynamic stimulations.

Consistent with our observation on NSC cultures in monolayer, *PDGF* promotes *Hes5* expression and proliferation in neurospheres (fig. S4E). However, observable transition in neurospheres happens later than monolayer cultures, only after stimulation for 2 days or more, possibly due to reduced transport of ligands to NSCs cells at the core of neurospheres. Due to such effect, we have focused on analyzing data collected from monolayer cell culture in our experiment rather than from neurospheres.

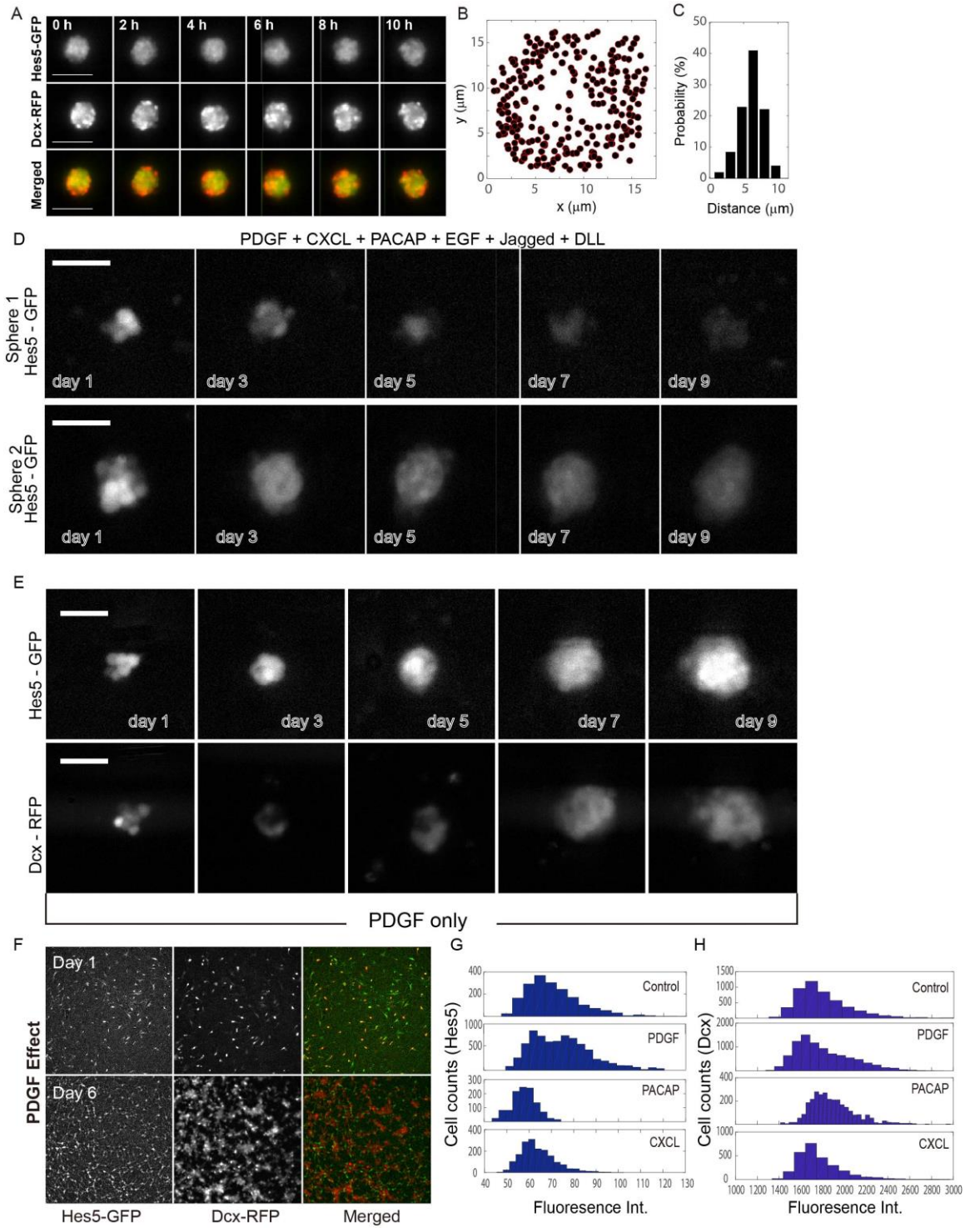

Fig. S4. *Hes5* and Dcx expression regulating NSC cellular behavior. (A) Fluorescence images showing organization of *Hes5*-high and *Dcx*-high cells within a NSCs sphere in our microfluidic experiments. (B) Positions of NSCs with high *Dcx* expression level in a sphere collected over a time span of 5 h, showing that most *Dcx* expressing cells are

position near the periphery (C) Probability of finding *Dcx*-high NSCs as a function of distance away from the sphere center. We found that within 10 hours culture on chip, NSC sphere rotated and showed a layered structure with *Hes5*-positive cells in the core and *Dcx*-positive ones at the outer layer. Scale bar in all images denote 40 um. (D) Time-course images of NSC spheres exposed to the combination of all 6 ligands in our chip indicate different ligand transport due to size differences. In the upper panel, we observe that when the sphere size is small (i.e. more efficient transport), *Hes5* expression level decreased dramatically and the neurospheres progress towards differentiation, which is the expected behavior in response to exposure to all 6 ligands. In the lower panel, larger NSC spheres showed higher *Hes5* levels at all time points, indicating limited exposure to the ligands due to limited transport effects. Scale bar is 40 μ m. (E) Development of NSC sphere exposed to *PDGF* stimulation. We observe that *PDGF* promote NSC sphere *Hes5* expression. Scale bar in all images denote 40 μm. (F) Sample fluorescent images from well-plate based experiments, showing NSC Hes5 and Dcx expression after incubation with PDGF for 6 days. Distribution of single NSC cell fluorescence intensity in (G) Hes5-GFP, and (H) Dcx-RFP channel after 6 days of stimulation with PDGF, PACAP and CXCL.

Section S5. Combinatorial and sequential experiments performed in 96-well plates

To validate outcomes from microfluidic cultures, we have performed experiments in 96-well plates under the same conditions that showed the most significant NSC cell fate changes in the microfluidic chip. These are:

1) Single ligand stimulation with PACAP and *PDGF* for 6 days (related Fig. 3C) ;

2) Combinatorial stimulation with *Jagged+EGF+PDGF* or *DLL+EGF+PDGF* for a total of 6 days (related Fig. 4A);

3) Sequential stimulation with the following sequences:

DLL>>EGF>>PDGF>>CXCL>>Jagged>>PACAP and

DLL>>PDGF>>CXCL>>Jagged>>PACAP>>*EGF* (Related to Fig. 4A)

In the well-plate sequential stimulation experiments, NSCs were cultured under each ligand for 1 day, for a total of 6 days, similar to the microfluidic experiments. NSCs maintained in regular culture medium were used as controls for each of these experiments. Below, we discuss the findings from the new well-plate experiments:

Single ligand stimulation experiments: Under *PDGF* stimulation (fig. S4F to S4H), the cell number of *Hes5*-high NSCs observed on day 6 is 9% higher than cell number of control group (*p*-value=3.36×10^{-190}, using Wilcoxon rank sum test). This result suggests that *PDGF* leads to maintenance of NSCs stemness and are consistent with our findings on the microfluidic chip (Fig. 3). The positive effect of *PDGF* on maintaining NSC stemness is further verified through measuring the distribution of single NSC fluorescence intensity (fig. S4G). With *PDGF* stimulation, the population of cells expressing high levels of *Hes5* (intensity value 75 and higher) expands noticeably as compared to the control experiments. We note that both PACAP and *PDGF* single ligands stimulation do not bring significant difference in NSC proliferation in well-plates as compared to the control and experiments performed on chip (fig. S5A).

Through averaging over all *Hes5* positive cells, we find that *PDGF* stimulation leads to ~ 20% increase in NSCs *Hes5* level, and PACAP leads to ~10% decrease in *Hes5* level (fig. S5A). Even though *Hes5* changes are not as large as those obtained on chip, the qualitative behavior (i.e. the direction of the change) agrees well with the microfluidic experiments. PACAP in well-plates does not induce the large change in cell growth observed in the microfluidic system. These differences are likely due to less frequency

media delivery (“feeding”) in well plates, which is a technical limitation of non-automatized well-plate experiments. Notably, *CXCL* brings no significant effect on NSCs proliferation, *Hes5* and *Dcx* expression level as compared to control experiments, which also coincides well with what we observed on chip.

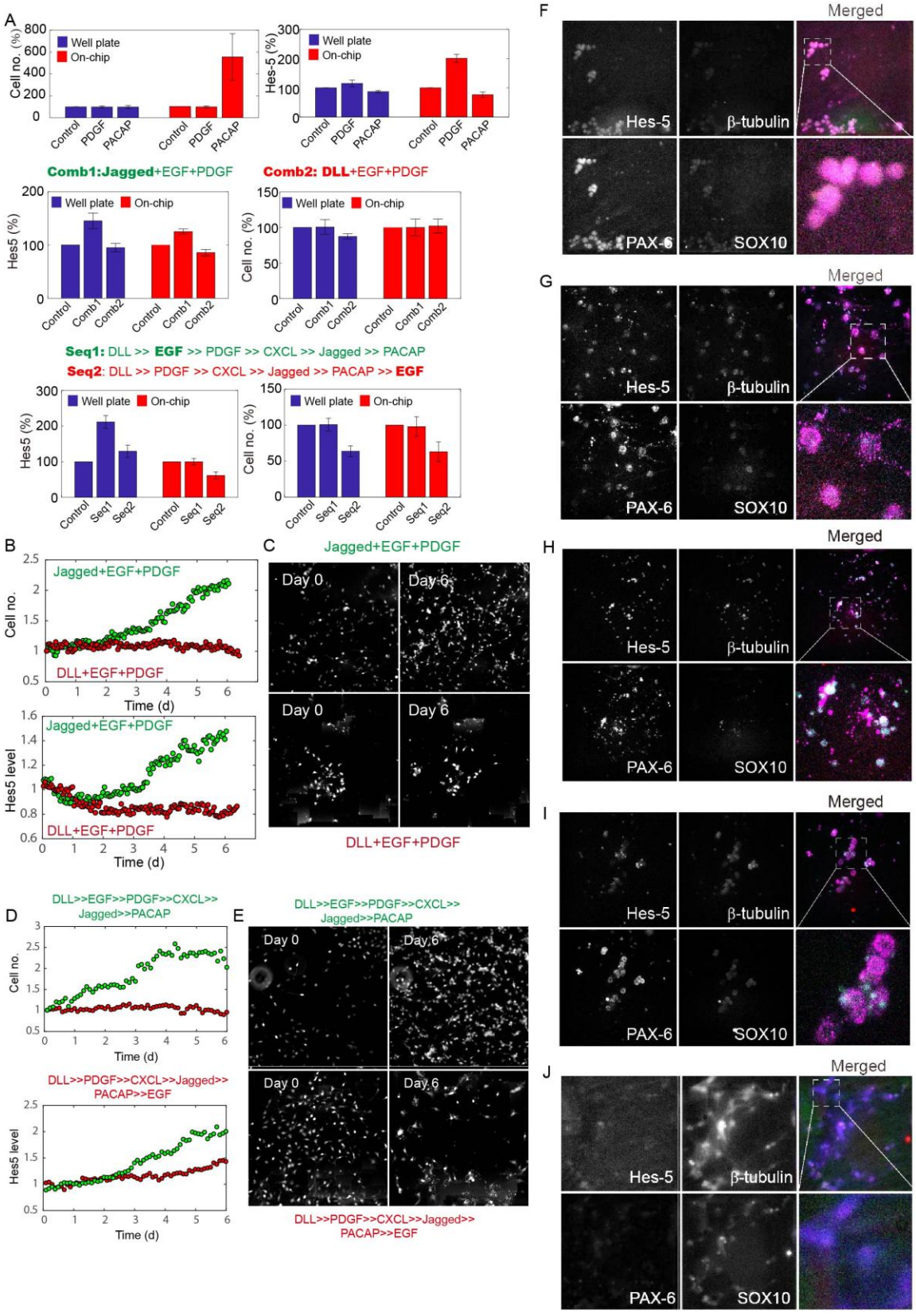
A
Cell no. (%)
Well plate
On-chip
Control
PDGF
PACAP
Hes-5 (%)
Comb1:Jagged+EGF+PDGF
Comb2: DLL+EGF+PDGF
Hes5 (%)
Cell no. (%)
Control
Comb1
Comb2
Seq1: DLL >> EGF >> PDGF >> CXCL >> Jagged >> PACAP
Seq2: DLL >> PDGF >> CXCL >> Jagged >> PACAP >> EGF
Control
Seq1
Seq2
B
Jagged+EGF+PDGF
DLL+EGF+PDGF
Cell no.
Hes5 level
Time (d)
C
Jagged+EGF+PDGF
Day 0
Day 6
DLL+EGF+PDGF
D
DLL>>EGF>>PDGF>>CXCL>>
Jagged>>PACAP
DLL>>PDGF>>CXCL>>Jagged>>
PACAP>>EGF
Cell no.
Hes5 level
Time (d)
E
DLL>>EGF>>PDGF>>CXCL>>
Jagged>>PACAP
Day 0
Day 6
DLL>>PDGF>>CXCL>>Jagged>>
PACAP>>EGF
F
Merged
Hes-5
β-tubulin
PAX-6
SOX10
G
Merged
Hes-5
β-tubulin
PAX-6
SOX10
H
Merged
Hes-5
β-tubulin
PAX-6
SOX10
I
Merged
Hes-5
β-tubulin
PAX-6
SOX10
J
Merged
Hes-5
β-tubulin
PAX-6
SOX10

Fig. S5. Combinatorial and sequential stimulation of six ligands regulating NSC self-renewal and differentiation. (A) In the top row, the variations in cell number and *Hes5* level after being stimulated with *PDGF* and PACAP for 6 days on-chip (blue) are plotted against parallel experiments performed in 96-well plate (red). Combinational (middle row) and sequential inputs (bottom row) experiments performed on-chip (blue) and in well-plate (red) are compared. (B) NSCs cell growth rate and Hes5 expression level measured in presence of combinations 'Jagged+EGF+PDGF' and 'DLL+EGF+PDGF' over the timespan of 6 days. We find that Jagged+EGF+PDGF enhances NSC self-renewal. (C) Fluorescent images showing NSCs Hes5 expression after incubation under combinatorial conditions for 6 days. (D) NSCs cell growth rate and Hes5 expression level accessed in presence of sequential inputs 'DLL>>EGF>>PDGF>>CXCL>>Jagged>>PACAP' and 'DLL>>PDGF>>CXCL>> Jagged>>PACAP>>EGF'. Ligands are replaced daily through pipetting. (E) Fluorescent images showing NSC Hes5 expression after incubation under sequential conditions for 6 days. NSCs were maintained in (F) regular culture medium, (G) PACAP, (H) PDGF, (I) CXCL and (J) Mixer of all 6 ligands including PDGF, CXCL, PACAP, DLL, Jagged and EGF, on chip for 6 days, and automatically stained on-chip with PAX6, Sox10 and β-III tubulin to access NSC self-renewal and differentiation. Immunostaining shows strong PAX6 signal. Selected areas, which are indicated by white squares, are enlarged for better illustration of immunostaining results. Together with the *Hes5* signal, we find that NSC stemness is well maintained during 6 days culture on chip under the control conditions. Related to Fig. 2E.

Combinatorial stimulation experiments: Combinatorial input *Jagged+EGF+PDGF* clearly promotes NSC self-renewal in the well plates (i.e. increased cell proliferation and increased *Hes5* expression level), and the replacement of *Jagged* by *DLL* induced dramatically different NSC responses, showing decreased NSC cell counts and *Hes5* expression (fig. S5B to S5E). These well plate results are similar to our microfluidic experiments (fig. S5A) and show that the replacement of a single ligand in a combinatorial input can completely change the direction that NSCs will take, verifying one of the most interesting findings from our study.

Sequential stimulation experiments: The input sequence '*DLL>>EGF>>PDGF>>CXCL>>Jagged*>>PACAP' promotes NSC proliferation and

Hes5 expression in well plates (fig. S5D and S5E). Positioning *EGF* on the 6th day, instead of 2nd day, reverses the effect of the input sequence on NSC proliferation, and diminishes the original enhancement on *Hes5* expression. The same effect of different sequences was also observed on microfluidic chip experiments (fig. S5A, S5D and S5E). Overall, we demonstrate that our findings obtained from microfluidic experiments can be qualitatively reproduced using standard cell culture methods using the well plate.

Section S6. Extended discussion of high-throughput combinatorial and sequential input studies

The microfluidic screening performed in our study are aimed at *in-vitro* recapitulation of the *in-vivo* signaling dynamics we recently measured during mouse brain development. These 6 selected ligands were chosen based on RNA-seq data collected from primary cells from the dorsal telencephalon of *Hes5::GFP* transgenic mice from embryonic day 10.5 to postnatal day PN (figures not included) (V. Taylor *et. al*, manuscript in preparation). We have undertaken an extensive transcriptional analysis of the gene expression by NSCs, basal progenitors and newborn neurons during corticogenesis in mice. The analysis of the gene expression profiles revealed that, Adcyap1, *CXCL*12, *DLL*1, Jag1, *PDGF*a, and the *EGF* receptor show significant and dynamic expression by NSCs throughout cortical development. These are the ligands or receptors of the ligands we tested in our microfluidic study. As some of these ligands are known to play an important role in NSC maintenance and differentiation, and others are potentially novel in this respect, we chose this combination to perform high-throughput microfluidic analysis of their combinatorial functions. The combinatorial analysis we show would not have been feasible *in vivo* or even in conventional culture systems.

As discussed above, our RNA-seq data from *Hes5::GFP* transgenic mice showed that during brain development, microenvironment housing NSC (niche) is highly dynamic. Composition of surrounding molecules (types and concentrations) is constantly changing, which we now believe play important roles in modulating cellular behavior. To get insights into effect of dynamic environmental conditions during biological processes (e.g. cerebral development, immune response), we develop a high throughput and biologically robust platform enabling systematic dissection of such processes in longitudinal cell culture experiments. Our study is aimed at direclty recapitulating the *in-vivo* measured dynamic signaling events by testing the effect of the same highly dynamic signaling molecules on NSC cell fate in a microfluidic format.

In this study, we demonstrate the importance of the environmental context and signal timing in NSC differentiation (Fig. 3 and 4). For example, NSCs are directed to either self-renewal (high *Hes5* expression) or differentiation (low *Hes5* expression) by changing only one ligand within the combination (*Jagged* to *DLL*, Fig. 4A). Similarly, changing the temporal order of a single ligand can direct NSCs to different cell fates (Fig. 4B): delivering *EGF* on day 2 led to high *Hes5* expression levels and unchanged cell numbers indicating maintenance of the stem cell pool, whereas moving the application of *EGF* to day 6 led to a significant reduction in *Hes5* expression indicative of differentiation. The data suggests that there exist an optimal route of signal input sequence leading to NSC self-renewal, *Jagged* (day1) >> *EGF* (day2) >> *CXCL* (day4).

Statistical analysis of this data revealed “cellular logic rules” determining cell fate. For example, we found that the presence of certain ligands (e.g. PACAP and *PDGF*) overrules others when directing stem cell differentiation. Secondly, cells at various decision points committed towards to either differentiation or self-renewal, and ignored the signals that come afterwards. Furthermore, increasing environmental complexity (i.e. increasing the number of ligands) generally suppressed NSC proliferation, however, reducing the input complexity seems to enhanced the stem cell pool.

Based on such reasoning and experimental design, we found that stem cell fate decision is highly dynamic depending on changing environmental conditions, and the effect of each participating ligand is often context-dependent, both in space and time. Our study emphasizes the needs to take systematic approach while studying early cerebral development, and an enabling platform (like our microfluidic system).

Section S7. *Hes5* expression as a valid marker for NSC stemness

We and others have shown extensively that *Hes5* expression strongly correlates with NSC potential (*12,16,21-24*). In the developing cerebral cortex, *Hes5* is restricted to the NSCs and represses neurogenesis through its repression of proneural gene expression. Hence, at the time points analyzed *Hes5* expression is restricted to NSCs. In addition, although it could be envisaged that activating Notch signaling could result in *Hes5* expression even in non-NSC cells, this seems not to happen at this developmental time point. Clearly the repression of proneural gene expression by *Hes5* and the requirement of the proneural transcription factors for neurogenic differentiation partially explains why

Hes5 positive cells do not express neuronal differentiation genes including *Dcx*. Conversely, some glia of the postnatal brain do express *Hes5* and which potentially reflects active Notch signaling. In our analysis and at the time-points we analyzed the activity of *Hes5* correlates with NSCs and their proliferative activity. We cannot formally exclude that prolonged exposure of the cells to Notch ligands in combination with other factors including *EGF* and *PDGF*a will not result in subsequent gliogenic differentiation. This would be interesting to analyze in detail in the future with our microfluidic system. In fig. S6G, we show that *Hes5*-GFP and *Dcx*-dsRed are exclusive using samples from embryonic brains at E13.5 and E15.5.

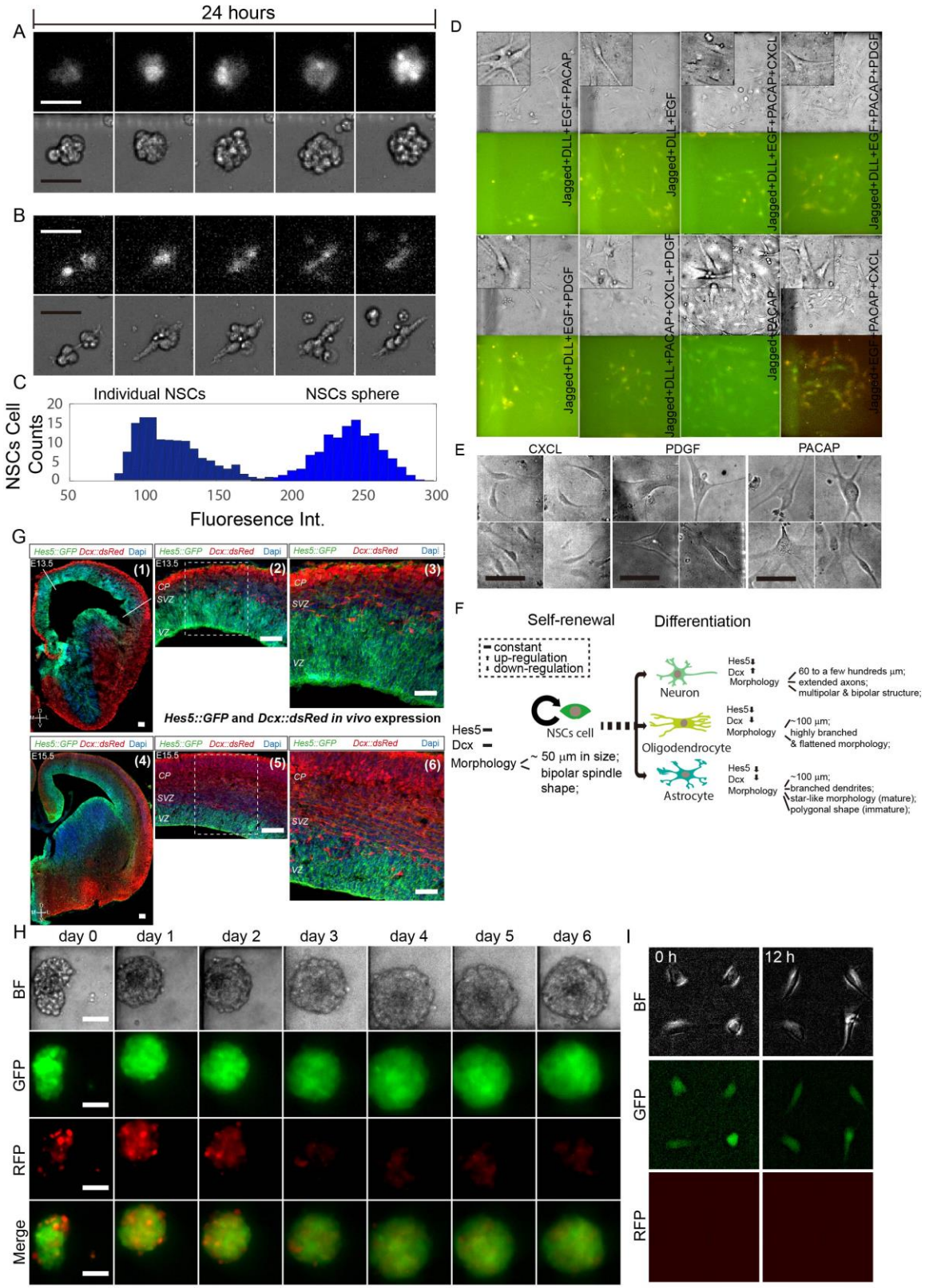
A
24 hours
B
C
Individual NSCs
NSCs sphere
NSCs Cell Counts
Fluoresence Int.
D
Jagged+DLL+EGF+PACAP
Jagged+DLL+EGF
Jagged+DLL+EGF+PACAP+CXCL
Jagged+DLL+EGF+PDGF
Jagged+DLL+PACAP+CXCL+PDGF
Jagged+PACAP
E
CXCL
PDGF
PACAP
F
Self-renewal
Differentiation
constant
up-regulation
down-regulation
Hes5
Dcx
Morphology
~ 50 μm in size; bipolar spindle shape;
NSCs cell
Neuron
Oligodendrocyte
Astrocyte
60 to a few hundreds μm; extended axons; multipolar & bipolar structure;
~100 μm; highly branched & flattened morphology;
~100 μm; branched dendrites; star-like morphology (mature); polygonal shape (immature);
G
Hes5::GFP Dcx::dsRed Dapi
Hes5::GFP and Dcx::dsRed in vivo expression
CP
SVZ
VZ
H
day 0
day 1
day 2
day 3
day 4
day 5
day 6
BF
GFP
RFP
Merge
I
0 h
12 h
BF
GFP
RFP

Fig. S6. Correlation between *Hes5* expression and NSC stemness. (A) NSCs with increased *Hes5* level aggregate and form spheres. Scale bars in all images denote 40 μm. (B) NSCs with decreased *Hes5* level remain as individual cells. Scale bars in all images denote 40 μm. (C) Distribution of NSCs *Hes5*-GFP fluorescence intensity within the spheres (light blue) and as individual cells (dark blue). (D) Fluorescence and bright field images of NSCs under selected conditions. (E) Bright field images of NSCs cultured on chip in media containing (from left to right) 200 ng/ml *CXCL*, 100 ng/mL *PDGF* and 500 nM PACAP. The scale bars are 50 μm in all images. (F) Schematic drawing of NSC differentiation determined by *Hes5* and *Dcx* expression level, and cell morphology. (G) *Hes5*::GFP labels NSCs in the ventricular zone and *Dcx*::dsRed labels newborn neurons in the intermediate zone and cortical plate. (1-3) Expression of *Hes5*::GFP and *Dcx*::dsRed at E13.5. The lines in A signify the regions micro-dissected for generating primary NSC cultures as neurospheres. (4-6) Expression of *Hes5*::GFP and *Dcx*::dsRed at E15.5. VZ-ventricular zone, SVZ- subventricular zone, IZ-intermediate zone, CP-cortical plate, E-embryonic day. Scale bar: 100 μm. (H) Real time tracking of a neurosphere in a 6 days stimulation and culture experiment. We observe that NSC cells that express high level of *Hes5*-GFP signal proliferate over weeks. Scale bars denote 50 μm in all images. (I) Neurospheres retrieved from cell culture chamber continue to grow in 96-well plate. The lack of *Dcx* signal among dissociated cells suggests *Hes5* as a good indicator for stemness.

First, we have shown extensively both *in vivo* and *in-vitro* that *Hes5*-GFP expression correlates with NSC potential and the undifferentiated state (*23*,*24*). We believe that at present, *Hes5*-GFP is one of the better if not the best reporter of undifferentiated NSCs (*12*,*16*,*21-24*). In addition, we have shown in the past that *Hes5*-GFP expression correlates better with the expression of other NSC markers such as Hes1, and that its expression is more restricted to NSCs than other markers in the developing dorsal cerebral cortex including Sox2 and Pax6 for example. In fig. S6G, we show that *Hes5* and *Dcx* can reflect NSCs self-renewal and differentiation during early embryonic days.

Sphere formation is one of the key features for stemness (*25, 26*). In our microfluidic cell culture experiments, we observe that NSCs that aggregate into neurospheres show elevated *Hes5* level compared to individual NSCs (fig. S6A to S6C), which validates

Hes5 as a marker for NSC stemness. This further indicates that activation of Notch signaling (increased *Hes5*) in neurospheres (*25*). Moreover, diameter of *Hes5* high NSC spheres nearly doubles within 24 hours, suggesting self-renewal of the stem cells. However, the cells with decreasing *Hes5* level mostly remain as individual cells (fig. S6B), or a sphere with no obvious increase in size (fig. S6C), which further supports *Hes5*'s role as a marker for self-renewal.

Section S8. Immunostaining on chip and determining NSC phenotypes

We performed experiments on our microfluidic platform with immunostaining of PAX6 (magenta, NSC stemness), Sox10 (red, differentiation towards Oligodendrocytes), and β-III-Tubulin (blue, differentiation towards neuron) under conditions with single ligands (fig. S5F to S5J) and investigated the correlation of these results to cellular phenotypes determined from measurements of *Hes5* (green, NSC stemness), *Dcx* and morphology.

Our results suggest that combined stimulation with all six ligands induce differentiation into neurons (high β-III-Tubulin expression, fig. S5J) within 6 days duration of our experiments. Stimulation experiments with single individual ligands show varying degrees of commitment to different lineages, but most NSCs did not fully differentiate to any cell lineage after 6 days stimulation with single ligands (fig. S5F to S5I). This is expected, because unlike hematopoietic stem cells (HSCs), whose morphological transition during differentiation is not only fast but also easily distinguishable, NSC differentiation takes longer time and is highly dynamic. We also found that NSCs

exposed to different combinatorial inputs show distinct morphological characters (fig. S6D to S6F), and the changes happen in a highly dynamical fashion.

Section S9. Statistical analysis of combinatorial and sequential results

A detailed description about the methodology of statistical analysis and multiple-test correction can be referred to section 1.5 above. In statistical analysis, we now calculate the median absolute deviation estimated via Hodge-Lehmann method to show the response variances of the conditions tested in our study.

First of all, it is worth to emphasize the difference between two experimental settings: combinatorial input experiments (the same ligand mixture condition are held for 6 days) versus sequential input experiments (ligands are replaced on a daily basis), because ligands can play seemingly contradictory roles. For instance, in the combinatorial experiments, altogether with *EGF* and *PDGF*, *Jagged* favors self-renewal with a 10% increase of *Hes5* expression with adjusted *p*-value 0.024 (Fig. 4A, the complete test results can be referred to the spreadsheet 'Combinatorial_Input' in the excel file: Table S2.xlsx). Whereas in the sequential experiment, *Jagged* was found to be pro-differentiative by driving a 5% decrease of *Hes5* expression with adjusted *p*-value 1.86×10^{-8}, if applied on the first day (The complete test results can be referred to the spreadsheet 'Sequential_Input' in the excel file: Table S2.xlsx).

Here, let us consider combinatorial treatment using cell count as outcome to illustrate the results. The effect size (percentage change) and BH-adjusted *p*-values associated with each condition are visualized in the bubble plot in fig. S8A. In the figure, only conditions with high significance or large effect sizes are annotated. As for the specific example of *PACAP*, it alone can increase cell number by 14% (adjusted *p*-value = 0.0015), giving rise to a subgroup for which the median of normalized cell count is 1.60 and median absolute deviation is 0.43 (Table S2). Complete test results can be referred to the spreadsheet 'Combinatorial_Input' in the excel file: **Table S2.xlsx**. In the same fashion, we generated bubble plots and tables for combinatorial measures on *Hes5* expression and *Dcx* expression (see fig. S8B and S8C and Table S2.xlsx).

Section S10. NSC single-cell tracking during combinatorial and sequential stimulation

Heterogeneity among NSCs has been observed. It is observed that there exist at least 2 cell lineages upon *PDGF* stimulation, with one (dominant) showing much higher cell growth rate compared to the other (Fig. 2C and D). However, as merely 3 out of ~ 50 cells distinguish themselves from the rest of the colony, our conclusion on *PDGF* effect is not affected or perturbed by such heterogeneity. Our study also reveals that *PDGF* helps to maintain NSC homogeneity at high doses (Fig. 2E). Low concentrations of *PDGF* actually promotes heterogeneity with prolonged incubation, as compared to control and other ligands. While, PACAP and *CXCL* bring no obvious increase in heterogeneity during stimulation at all doses.

NSC heterogeneity in *Hes5* and *Dcx* level can be caused by numerous factors like cell morphological change during migration, cell division and cell-cell contact. Among the few cells, which we manage to track for 6 days during stimulation, NSC single cells develop following the same route as the population (fig. S7A and S7B), despite of the fluctuation in *Hes5* and *Dcx* level.

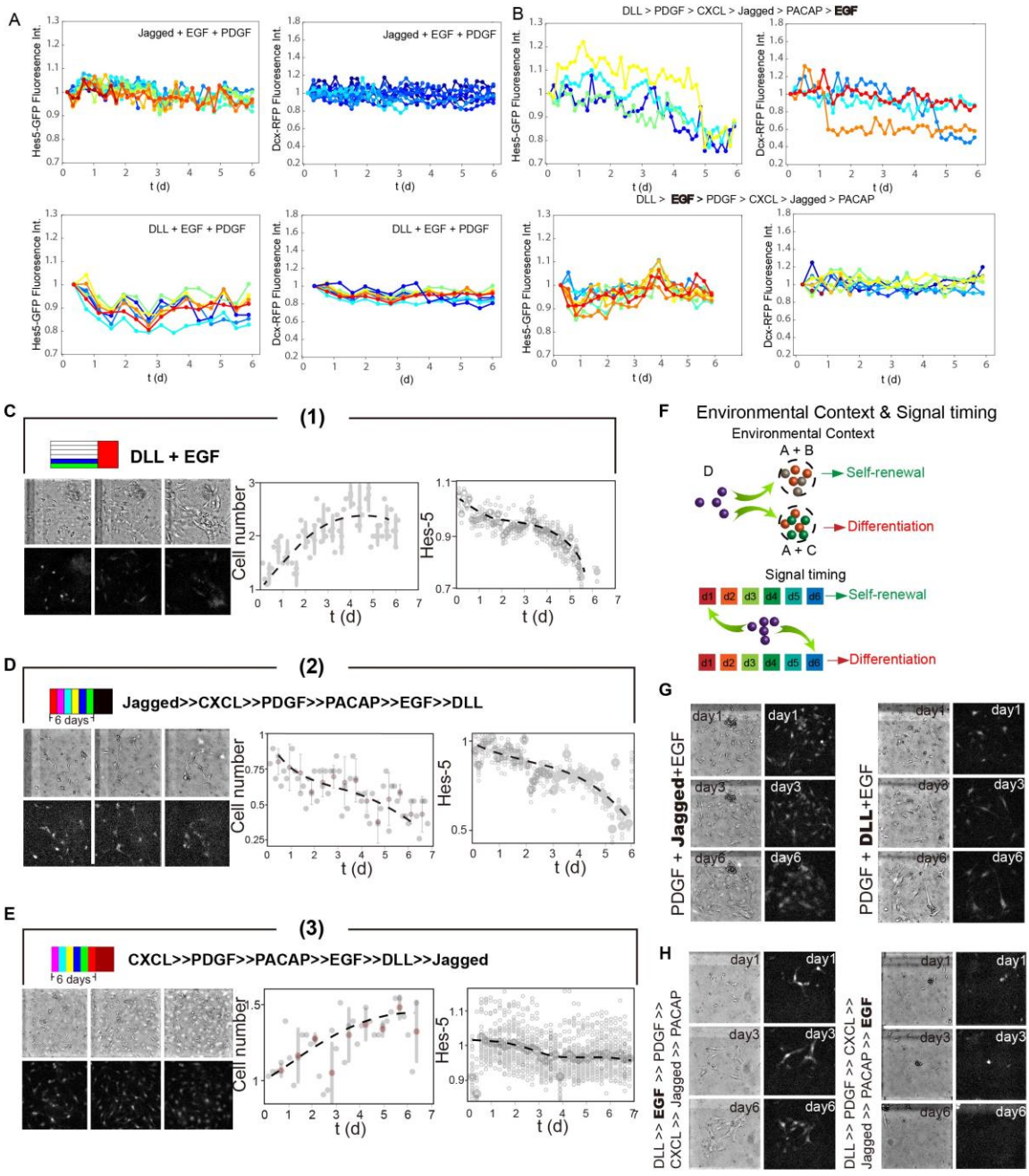

Fig. S7. Combinatorial and sequential inputs regulating NSC proliferation, *Hes5*, and Dcx expression. Single NSC cell tracking showing real-time *Hes5* and *Dcx* expression during 6 days stimulation with, (A) combinatorial inputs: *Jagged+EGF+PDGF* and *DLL+EGF+PDGF*. Related to Main Fig. 4A; (B) sequential input, *DLL>>PDGF>>CXCL>> Jagged*>>PACAP>>*EGF* and *DLL>>EGF>>PDGF>>CXCL>> Jagged*>>PACAP. Related to Main Fig. 4A. (C-E) Example data sets from one experiment. The selected stimulation conditions are shown, including (1) DLL + EGF, (2) Jagged >> CXCL >> PDGF >> PACAP >> EGF >> DLL, and (3) CXCL >> PDGF >> PACAP >> EGF >> DLL >> Jagged. These conditions (marked with white squares in Fig. 3B) show the variation in cell proliferation and Hes5

expression dynamics. All cell images are 400 μm by 400 μm in area. (F-H) Schematic drawing shows the importance of environmental context and signaling timing in determining NSC cell fate. Single NSC tracking images, and dynamic changes in cell number and Hes5 level are plotted for two ligand combinations containing (Jagged, PDGF, EGF) and (DLL, PDGF, EGF); and 2 select ligands sequences (DLL >> EGF >> PDGF >> CXCL >> Jagged >> PACAP) and (DLL >> PDGF >> CXCL >> Jagged >> PACAP >> EGF). All cell images are 400 μm by 400 μm in area.

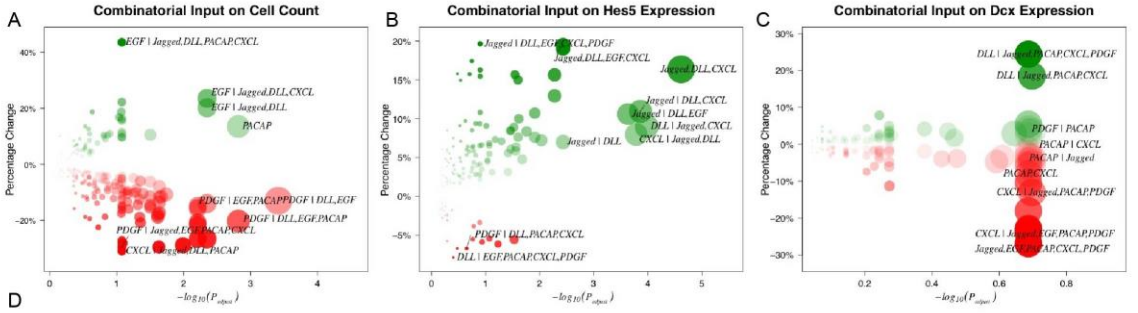

D

	Day 1			Day 2			Day 3			Day 4			Day 5			Day 6		
	Cell Count	Hes5	Dcx	Cell Count	Hes5	Dcx	Cell Count	Hes5	Dcx	Cell Count	Hes5	Dcx	Cell Count	Hes5	Dcx	Cell Count	Hes5	Dcx
Jagged	+9%**	-5%***	+5%**	–	+3%***	–	–	+6%***	+5%*	–	–	-5%**	–	–	–	–	–	–
DLL	-7%*	–	+8%***	–	+5%***	–	–	+4%***	–	–	-2%*	–	–	-3%***	–	–	-3%***	–
EGF	–	-8%***	–	–	–	–	+8%*	–	–	–	–	+4%*	-8%*	+3%***	–	–	+3%***	–
PACAP	+16%***	-4%***	-8%***	-11%***	–	–	–	–	–	–	–	–	–	+3%**	–	–	+3%**	–
CXCL	–	+5%***	–	–	-4%***	–	–	-4%***	–	–	–	–	–	–	–	–	–	–
PDGF	-14%***	+11%***	–	+11%**	-2%**	–	–	-5%***	–	–	–	–	–	–	–	–	-2%*	–

	Cell Count	Hes5	Dcx
Jagged	-6%*	–	–
DLL	–	–	–
EGF	–	–	–
PACAP	+14%**	–	–
CXCL	-6%*	–	–
PDGF	–	+3%*	–

Fig. S8. Effect of various stimulation conditions on NSC cell fate subjected to statistical analysis. Wilcoxon rank sum test results for experiments that measured NSC (A) cell counts, (B) *Hes5* expression, (C) *Dcx* expression, under combinatorial inputs, visualized via a bubble diagram. The effect size (percentage change) and adjusted *p*-values associated with each condition are represented by colored bubbles, of which the diameter is proportional to negative log scale of adjusted *p*-value, and the color reflects percentage change (green for a positive percentage change and red for negative, and its opacity is proportional to the absolute scale). (D) Effect of single ligands effect during sequential (in the upper panel) and combinatorial (in the lower panel) experiments. The statistical analysis of cell count, Hes5 and Dcx expression using all 720 sequential and 63 combinatorial experiments are obtained via Wilcoxon rank sum test and summarized in the table. The 'promote'(green) and 'inhibitory' (red) effect of selected single ligands are listed for clarification.

Captions for Tables S1, S2 and Movies S1 to S5

Table S1. Microenvironment exposed to six single ligands and combinatorial and sequential ligand inputs (note: the order of the ligands in the table represents the order of ligands introduced into the microenvironments on daily bases). Number 7 denotes *Jagged*; 8 *DLL*; 9 *EGF*; 10 PACAP; 11 *CXCL*; 12 *PDGF*.

Table S2. Statistical analysis results associated with sequential and combinatorial inputs of six ligands based on cell count measurements and *Hes5* and *Dcx* expression level.

Movie S1. COMSOL simulation and time-lapse video of fluid exchange in a unit chamber on the chip. In the left panel, COMSOL simulation of flow profile within the cell culture chamber when being flashed under 2 different modes. In the right panel, a video demonstrates the operation of 1,500 individually addressable culture units.

Movie S2. Re-distribution of GFP after medium exchange and all valves are closed.

Movie S3. Retrieval of adherent cells (3T3, left) and suspension-cultured cells (Jurkat, right) from the chip.

Movie S4. Stimulation of 3T3 cells by sinusoidal TNF-α inputs.

Movie S5. Cell tracking videos of NSC spheres (top) and monolayer (bottom).